

# Droplet Size Evolution During Coalescence in Semiconcentrated Model Blends

I. Vinckier and P. Moldenaers

Dept. of Chemical Engineering, K. U. Leuven, 3001 Leuven, Belgium

A. M. Terracciano and N. Grizzuti

Dept. of Chemical Engineering, Università di Napoli Federico II, 80125, Napoli, Italy

*The droplet-size evolution in polymer blends, due to flow-driven coalescence, is investigated both experimentally and theoretically. In the experiments, preshearing at a high rate is applied to generate a fine morphology in the blend; subsequently, the shear rate is suddenly decreased to induce coalescence, and the resulting growth in droplet size is measured. It is demonstrated that rheological as well as microscopic techniques can be used for an in-situ determination of the size evolution of the droplets. Effects of shear rate, step-down ratio, and blend concentration were studied systematically. A master curve for the droplet growth at each step ratio can be obtained by plotting the relative increase in droplet diameter vs. the strain after step-down in shear rate, multiplied by the fraction of the disperse-phase squared. To model the droplet-size evolution the strategy of Chesters is followed. It is implemented here for semiconcentrated blends, resulting in a one-parameter model equation that correctly describes the experimental observations.*

## Introduction

Two-phase polymer blends constitute a material class of increasing importance. By blending, desirable properties of different polymers can be combined in a single, heterogeneous material. The microstructure strongly affects the characteristics of the blend. Therefore, controlling the morphology development during processing is of great importance. As in all emulsions, flow-induced changes of the structure in two-phase polymer blends are caused by two different phenomena: breakup and coalescence. The latter, which has received relatively little attention in the literature, is the subject of this article.

Flow-driven coalescence in emulsions is usually studied by decoupling the process in an external and an internal flow. The external flow is the macroscopic flow that brings the droplets together, and hence governs the collision frequency, the contact force, and the interaction time. The drainage of the fluid film between colliding droplets constitutes the internal flow. This film drainage is considered to be the critical step in the merging process of two colliding droplets. A comprehensive treatment of the subject has been given by

Chesters (1991). Depending on the interfacial mobility—fully mobile, partially mobile, and immobile interfaces—three models are available for the film drainage between a pair of colliding droplets. These models all treat this film as parallel sided and assume simple boundary conditions, such as a constant interaction force. In spite of the various approximations involved, their predictions are in good agreement with the numerical solution of the fully coupled problem of interfacial deformation and film flow (Chesters, 1991). The probability  $P$  of coalescence upon collision of two droplets is expressed as

$$P = \exp\left(-\frac{t_{\text{drain}}}{t_{\text{int}}}\right), \quad (1)$$

where  $t_{\text{drain}}$  is the time required for drainage of the fluid film between the droplets, and  $t_{\text{int}}$  is the interaction time during collision. A cruder, but physically sound assumption is that coalescence becomes impossible when the time needed for film drainage exceeds the interaction time between two colliding droplets, that is  $P = 0$  for  $t_{\text{int}} < t_{\text{drain}}$ , whereas  $P = 1$  for  $t_{\text{int}} \geq t_{\text{drain}}$  (Elmendorp and Van der Vegt, 1989; Janssen,

Correspondence concerning this article should be addressed to P. Moldenaers.

1993). Such a binary assumption for the coalescence probability introduces an upper limiting droplet size  $d_{ss}$ , above which coalescence is unlikely to happen.

Experimental studies on flow-induced coalescence in polymer blends under well-defined flow conditions are scarce. Only S ndergaard and Lyngaae-J rgensen (1996) have published quantitative data on droplet-size evolution due to coalescence under shear flow. The set of data published by these authors, however, is too limited to be used for verification of existing coalescence theories. The coalescence models mentioned earlier have been assessed by means of the steady-state droplet sizes obtained in polymer blends after sufficiently long shearing (Minale et al., 1997a,b; Grizzuti and Bifulco, 1997). Under conditions where breakup is not possible, that is, for a capillary number well below the critical value for breakup, a coalescence-limited droplet diameter,  $d_{ss}$ , was observed. The best agreement between experimental results and theoretical predictions for  $d_{ss}$  has been obtained by using the drainage model for partially mobile interfaces (Minale et al., 1997a,b), at least for blends with component viscosities of the same order of magnitude. Although the limiting droplet size is described quite well by this theory, there is no experimental evidence that the kinetics of droplet-size evolution are also correctly predicted. Starting from the approach suggested by Chesters (1991), the evolution of particle size due to coalescence is modeled here. Only the drainage model for partially mobile interfaces is considered. Subsequently, the evolution of the droplet size will be investigated experimentally, by rheological as well as microscopic techniques. The experimental results will then be used to evaluate the accuracy of the model predictions.

## Modeling of the Coalescence Process

For a monodisperse blend, the rate of change of the specific interfacial area,  $Q$ , can be expressed quite generally as (Chesters, 1991)

$$\frac{dQ(t)}{dt} = C(t)P(t)\Delta S(t), \quad (2)$$

where  $C(t)$  denotes the collision frequency per unit volume;  $P(t)$  is the coalescence probability, or the fraction of collisions that actually leads to coalescence; and  $\Delta S(t)$  is the change in interfacial area due to a single coalescence event. The latter, which is time-dependent through its dependence on droplet size, is based on the conservation of volume; expressions for  $C(t)$  and  $P(t)$  are discussed below.

As Chesters (1991), we start from the Smoluchowski equation (Smoluchowski, 1917) to calculate the collision frequency per unit volume. Assuming that the droplets follow the macroscopic shear flow, this equation is given by

$$C(t) = \frac{2}{3} \dot{\gamma} d(t)^3 n(t)^2, \quad (3)$$

where  $\dot{\gamma}$  is the shear rate;  $d(t)$  the droplet diameter; and  $n(t)$  the number of droplets per unit volume. Because hydrodynamic interactions are ignored in this expression, it should only apply to rather dilute systems. The coalescence probability

$P(t)$  is given by Eq. 1 where the interaction time is set as  $1/\dot{\gamma}$  and an approximate expression of  $t_{\text{drain}}$  for a single pair of droplets with partially mobile interfaces is taken from Chesters (1991):

$$P(t) = \exp \left[ -0.07655 \frac{p}{h_c} \left( \frac{\eta_m \dot{\gamma}}{\alpha} \right)^{3/2} d(t)^{5/2} \right]. \quad (4)$$

In Eq. 4  $p$  and  $\alpha$  are, respectively, the viscosity ratio (droplet over matrix viscosity) and the interfacial tension of the system;  $\eta_m$  is the matrix viscosity; and  $h_c$  is the distance between the droplets at which coalescence occurs spontaneously. This critical thickness is a weak function of droplet size (Chesters, 1991), but often this dependence is neglected (Elmendorp and Van der Vegt, 1986).

Combining Eqs. 2, 3, and 4 and expressing  $Q(t)$ ,  $\Delta S(t)$ , and  $n(t)$  in terms of volume fraction of the disperse phase  $\phi$  and droplet diameter (the details are given in the Appendix), results in the following differential equation for the evolution of droplet size:

$$\frac{dd(t)}{dt} = 0.525 \phi \dot{\gamma} d(t) \exp \{ -[m \cdot d(t)]^{5/2} \dot{\gamma}^{3/2} \}, \quad (5)$$

where

$$m = 0.358 \left( \frac{p}{h_c} \right)^{2.5} \left( \frac{\eta_m}{\alpha} \right)^{3/5}. \quad (6)$$

When breakup processes are ignored, Eq. 5 would predict an unbounded increase in the droplet size during shear. The growth rate, however, slows down dramatically because the probability of coalescence upon collision decreases strongly with size (Eq. 4). Experimentally, the droplet size will be regarded as a steady-state value ( $d_{ss}$ ) when its relative increase over a long shearing time, or rather over a large shear strain, is negligible:

$$\frac{\Delta d}{d} = 0.525 \phi \exp \{ -(m \cdot d)^{5/2} \dot{\gamma}^{3/2} \} \ll 1. \quad (7)$$

The choice of the numerical value at which the lefthand side of Eq. 7 is considered negligible is arbitrary, but it is kept fixed within the experimental protocol. This degree of arbitrariness is inherent in a pseudo steady state that is an experimental rather than a physical limit. By rewriting Eq. 7, an expression for the pseudo-steady-state droplet size is obtained:

$$d_{ss} = c \frac{\dot{\gamma}^{-3/5}}{m}, \quad (8)$$

where  $c$  is a function of the volume fraction of the blend, the numerical value of which depends on the experimental protocol. In the literature,  $d_{ss}$  is often given as (Chesters, 1991)

$$d_{ss} = \frac{\dot{\gamma}^{-3/5}}{m}, \quad (9)$$

which is the result of assuming  $P = 0$  for  $t_{\text{int}} < t_{\text{drain}}$  and  $P = 1$  elsewhere. This arbitrary binary approximation of  $P$  is rather crude and will not be used here.

An equation for the droplet diameter as a function of shearing time can be obtained by integration of Eq. 5:

$$\int_m^{\dot{\gamma}^{1/5} d(t)} \frac{du(t)}{0.525u(t) \exp[-u(t)^{5/2}]} = \phi \dot{\gamma} t, \quad (10)$$

where

$$u(t) = m \dot{\gamma}^{3/5} d(t). \quad (11)$$

Apart from the initial droplet size  $d_0 = d(t=0)$ , Eq. 10 contains only the unknown parameter  $h_c$  (through  $m$ , see Eq. 6), which can be used to fit the experimental data. In some of the present experiments, the initial morphology is given by the experimental limiting droplet size at the initial shear rate, as derived from Eq. 8. Introducing this result in Eq. 10:

$$\int_{c(\dot{\gamma}/\dot{\gamma}_0)^{3/5}}^{c[d(t)/d_0](\dot{\gamma}/\dot{\gamma}_0)^{3/5}} \frac{du(t)}{0.525u(t) \exp[-u(t)^{5/2}]} = \phi \dot{\gamma} t. \quad (12)$$

This equation predicts that the evolution of droplet size after a step-down in shear rate is a function of only three parameters: strain, step-down ratio, and blend concentration. The latter parameter appears on the righthand side of Eq. 12, and in the value of  $c$ . It should be mentioned that the assumptions that have been made to derive this equation restrict its application to rather dilute systems. Apparently, the viscosity ratio of the blend does not seem to play a role, but it should be noted that the basic assumption of partially mobile interfaces is only suitable for viscosity ratios around 1. Consequently, for blends with the same concentration, the following scaling behavior is predicted:

$$\frac{d(t)}{d_0} = f\left(\dot{\gamma} t, \frac{\dot{\gamma}}{\dot{\gamma}_0}\right). \quad (13)$$

It is emphasized again that this scaling relation was derived assuming that the initial droplet size obeys Eq. 8 with respect to the initial shear rate.

## Materials and Methods

### Materials

All experiments were performed on model blends of polyisobutene (PIB; Parapol 1300 from Exxon) dispersed in polydimethylsiloxane (PDMS; Rhodorsil 47V200.000 from Rhône-Poulenc). At the test temperature of 23°C the viscosity ratio is about 0.5 and the interfacial tension is 3 mN/m (Sigillo et al., 1997). With this system, the measurements can be performed at room temperature, thus avoiding problems of thermal degradation as encountered with real polymer melts as well as problems caused by the presence of solvents

in polymer solutions. Four blend concentrations were investigated with the volume fraction of the disperse phase ranging from 0.025 to 0.2. They are labeled as 2.5/97.5, 5/95, 10/90, and 20/80, where the first number represents the percent volume fraction of PIB and the second number the complementary PDMS content. The blends with up to 10% of disperse phase could be investigated by optical microscopy, whereas the 10/90 and 20/80 blends were more suitable for rheological measurements. Details of the preparation techniques and the steady-state rheology and morphology of these systems can be found elsewhere (Grizzuti and Bifulco, 1997; Vinckier et al., 1996).

### Experimental procedure

The experimental procedure is based on the existence of a hysteresis region in the size/shear-rate domain, as shown in Figure 1. Such a representation has already been used by Elmendorp and Van der Vegt (1986) and by Janssen (1993) and Janssen and Meijer (1995) to explain the possible morphologies in liquid-liquid dispersions. At each shear rate there is a minimum droplet size below which no breakup occurs. This critical size is characterized by a critical capillary number (Grace, 1982). On the other hand, the coalescence model, based on a partially mobile interface, predicts that coalescence slows down a great deal for large droplet sizes. The assumption that no coalescence can occur when the time for film drainage exceeds the interaction time of the colliding droplets, leads to an upper-limit droplet size for the coalescence process (Eq. 8). This equation still contains the fitting parameter  $h_c$ , which can be derived from the steady-state droplet sizes. The shear rate at the intersection of the curves,  $\dot{\gamma}_c$ , separates two regimes: for  $\dot{\gamma} > \dot{\gamma}_c$ , the final droplet size is the result of a dynamic equilibrium between breakup and coalescence; for  $\dot{\gamma} < \dot{\gamma}_c$ , a morphological hysteresis is possible (Minale et al., 1997a). Since the objective of the present experiments is to probe the morphology evolution due to coa-

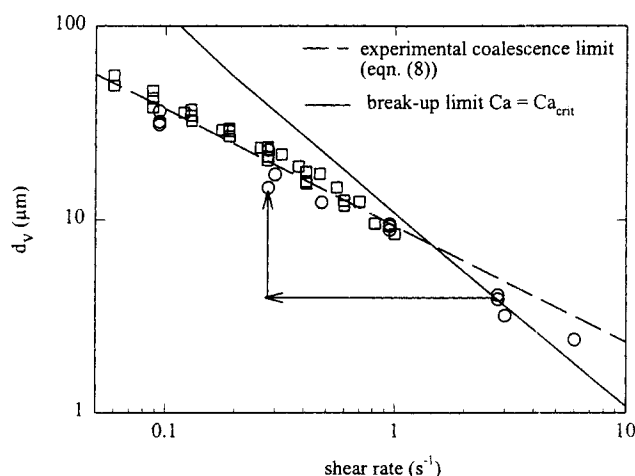


**Figure 1. Steady-state droplet size as a function of shear rate for the 10/90 blend.**

Squares: microscopic observations; circles: rheological results. The limiting droplet sizes for coalescence, given by Eq. 8 with  $h_c = 15$  nm and  $c = 2.4$ , and breakup, determined by  $Ca_{\text{crit}}$  (Grace, 1982), are added for comparison. The arrows represent a step-down experiment.

lence only, breakup phenomena should be avoided. This can be achieved once the hysteresis region has been identified by preshearing the blend at a high rate to generate a fine morphology, then stepping down to a shear rate below  $\dot{\gamma}_c$ . Breakup will not occur in this case since the droplet size will reach the coalescence limit before the breakup limit has been reached. A typical coalescence test is displayed by the arrows in Figure 1.

To probe the size of the disperse phase during the coalescence process, the following procedure was adopted. After the step-down in shear rate, the flow was intermittently stopped. At that stage the diameter of the disperse phase was determined either by microscopic observation or by a rheological experiment (see below), after which the flow was resumed immediately. It was verified that this "stop-and-go" procedure did not interfere with the shear-induced morphology evolution and that neither sedimentation (due to a small density difference between the two polymers) nor radial migration were present (see also Grizzuti and Bifulco, 1996).

The microscopic experiments were performed on an apparatus developed at the University of Naples, details of which are given by Grizzuti and Bifulco (1996). The shear cell consists of two parallel glass plates, which can be moved independently by two computer-controlled step motors. Images of the drops are obtained by a B/W CCD camera (Hitachi KP-ME1,  $768 \times 493$  pixels), attached to a microscope tube. Three objectives ( $10\times$ ,  $20\times$ , and  $32\times$  magnification) were used, depending on the size of the dispersed phase. Images were recorded on tape for later analysis, which was carried out by a PC-hosted frame grabber (Data Translation DT-2867-LC) equipped with a suitable software (Global Lab Image by Data Translation). A population of about 150 droplets was measured. From the analysis of this droplet population, average quantities such as number-average and volume-average drop diameter and distribution spread (standard deviation) could easily be derived. Quantitative analysis of the microscopic images was possible for blends with up to 10% disperse phase, sheared at rates below  $1 \text{ s}^{-1}$ . At higher shear rates the droplets were too small to be measured, and blends with more than 10% disperse phase were too turbid for an accurate size measurement.

The rheological technique is based on oscillatory measurements at small amplitudes. The results of such a test are very sensitive to the actual morphology of the blend as created by the preceding flow. By fitting the results of such measurements with the model of Palierne (1990), the volume average droplet diameter is obtained. This procedure has proven to be adequate in determining the steady-state morphology in immiscible blends of nearly inelastic polymers (Vinckier et al., 1996). Here, the procedure is used to determine the droplet size at different stages during the coalescence process. The experiments were stopped when the average droplet size reached half the minimum gap size between the cone and the plate, since deviatoric results were obtained beyond that point. The tests have been performed on a dynamic stress rheometer (DSR; Rheometric Scientific), a stress-controlled rheometer which is able to apply an oscillatory stress as well. A cone and plate geometry with a radius of 12.5 mm and a cone angle of 0.1 rad has been selected. This setup provides a uniform shear rate throughout the sample; the temperature was kept constant at  $23.0^\circ\text{C}$  by means of a Peltier element.

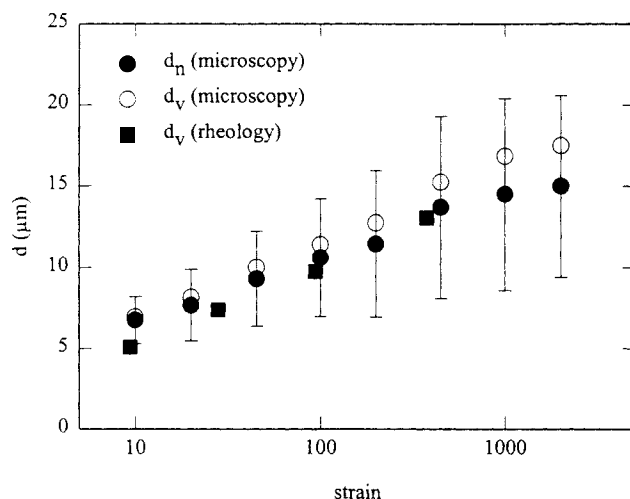


**Figure 2.** Evolution of the average droplet size in the 10/90 blend after step-down from  $3.0$  to  $0.3 \text{ s}^{-1}$ .

The error bars represent twice the standard deviation of the droplet size distribution.

## Results and Discussion

Figure 2 shows the results of the stepdown experiment from  $3 \text{ s}^{-1}$  to  $0.3 \text{ s}^{-1}$ , indicated by the arrows in Figure 1. The droplet size in a 10/90 blend is plotted versus  $\dot{\gamma}t$ , that is, the total strain applied after the step-down in shear rate. Optical microscopy allows one to monitor the whole distribution of droplet sizes as a function of time. This morphological information is shown in Figure 2 as the numerical mean diameter  $d_n$ , with error bars having a width that corresponds to twice the standard deviation of the distribution. The volumetric average drop diameter is plotted as well, to make a comparison possible with the rheological measurements, which only give this average value. It is obvious that coalescence occurs, as the average size increases with time. It should be pointed out that the coalescence rate slows down continuously but does not come to a stop, as outlined in the section on modeling. Coalescence does not only generate a larger average droplet size, but produces a widening of the size distribution as well. For the test displayed in Figure 2 this widening remains limited: the maximum ratio of the volume average over the number average droplet size is below 1.3. Good agreement is observed between the results of the two different techniques. The diameter measured by optical microscopy in the early stages of coalescence is, however, systematically larger than the one obtained from rheology. Such a discrepancy is most probably related to the small drop diameter created at the initial shear rate of  $3 \text{ s}^{-1}$ . Due to the high turbidity of the sample under these conditions, optical microscopy is not able to detect the smallest droplets, leading to an overestimation of the average size.

The effect of initial and final shear rate on the coalescence kinetics has been investigated systematically. The results of various tests plotted as scaled diameter vs. strain are shown in Figure 3. The solid lines, corresponding to model predictions, are discussed later. Since microscopy suffers from considerable error in detecting small droplets, the initial droplet size as derived from the rheological measurements has been used to scale the microscopic data. This explains why the mi-

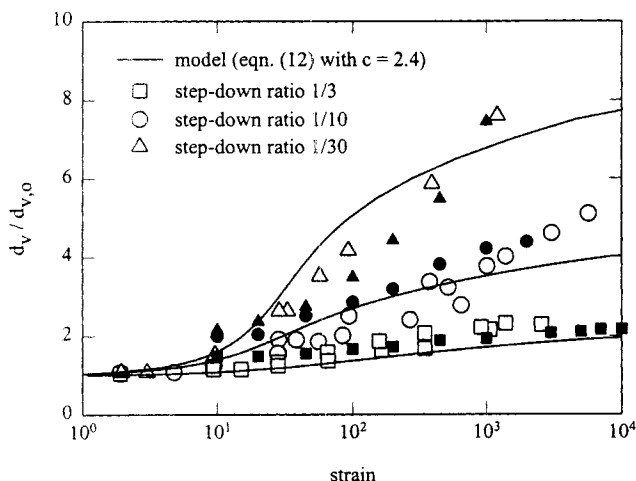


**Figure 3. Droplet-size evolution in the 10/90 blend during experiments with different step-down ratios and various initial shear rates.**

Step-down with ratio 1/30 from initial shear rates of 4.5 and 3.0  $\text{s}^{-1}$ ; ratio 1/10 from 4.5, 3.0, 1.0, and 0.5  $\text{s}^{-1}$ ; and ratio 1/3 from 4.5, 3.0, and 0.3  $\text{s}^{-1}$ . Microscopic (filled) and rheological (open) measurements; solid lines: predictions of Eq. 12.

croscopy results do not tend to one in the limit of small strain. Nevertheless, the overall agreement between rheological and microscopic data is considered to be good. Moreover, the data obey well the scaling relationship represented by Eq. 13: the curves of scaled diameter for a constant value of step-down ratio are superimposed when plotted vs. strain. This scaling behavior is also consistent with the model of Doi and Ohta (1991), originally proposed for cocontinuous 50/50 mixtures of immiscible liquids with the same viscosity. These authors predict that, for stepwise changes in shear rate, the morphological parameters (specific interfacial area  $Q$  and interface tensor  $q_{ij}$ ), divided by their initial value, depend only on strain and step ratio. For the specific interfacial area this scaling relation can be written as

$$\frac{Q(t)}{Q_0} = f\left(\dot{\gamma} \cdot t, \frac{\dot{\gamma}}{\dot{\gamma}_0}\right). \quad (14)$$

Although various assumptions have been made, the scaling relation is independent of some of these assumptions and should hold quite generally for systems that include no intrinsic length scale (Doi and Ohta, 1991). For almost spherical droplets in a continuous matrix one can assume that the specific interfacial area is inversely proportional to the size of the droplets. In that case, the Doi-Ohta scaling for step-down tests is equivalent to Eq. 13, although a different assumption is used for the initial droplet size. The Doi-Ohta scaling relation is based on an inverse proportionality between the initial length scale of the system, that is,  $Q_0^{-1}$  or  $d_0$ , and the initial shear rate, which would result for a breakup-determined morphology. For shear rates above the critical value, the blends under investigation have no intrinsic length scale because the droplets size results from the kinetics of the sys-

tem and the Doi-Ohta scaling should apply. For shear rates below the critical value the experimentally attainable droplet size is limited by coalescence (Eq. 8), so Eq. 13 applies, which entails the same scaling property.

The experimental observations can also be used to evaluate quantitatively the accuracy of the coalescence model presented in this article. In Figure 4, the predictions for the evolution of droplet size are compared with the experimental results. As an example, the data of Figure 2 are replotted together with the model curve calculated from Eq. 10. This equation contains two unknown parameters:  $m$  (or rather  $h_c$ ) and the initial droplet size  $d_0$ . Good correspondence with the experimental results is obtained by fitting  $h_c$  and using the experimental value for  $d_0$ . Some comments on  $h_c$  are necessary. In the original work of Chesters (1991)  $h_c$  is defined as a critical thickness at which the fluid film between a single pair of colliding droplets becomes unstable:

$$h_c \approx \left( \frac{Ad}{16\pi\alpha} \right)^{1/3}, \quad (15)$$

where  $A$ , the Hamaker constant, depends on the fluids concerned (typically  $A \sim 10^{-20}$  J). For droplet diameters around 10  $\mu\text{m}$  this equation predicts a critical rupture thickness of about 10 nm. However, by making  $h_c$  an adjustable parameter for describing coalescence in semiconcentrated blends, this physical meaning is lost because its value thus includes concentration effects (Minale et al., 1997a,b). Nevertheless, the best fit for all coalescence curves of the 10/90 blend (15 nm) is of the same order of magnitude as theoretically expected. On the other hand, a value of 200 nm for  $h_c$  has been reported for this system (Grizzuti and Bifulco, 1996) which was obtained by microscopic observation of only the pseudo-steady-state droplet sizes instead of the droplet-size evolution. Moreover, these authors applied the binary approximation of  $P$  for fitting their data (Eq. 9), which inherently gives a value for  $h_c$  that is a factor  $c^{5/2}$  larger than using the full expression for  $P$  (Eq. 8). Applying their fitting procedure to

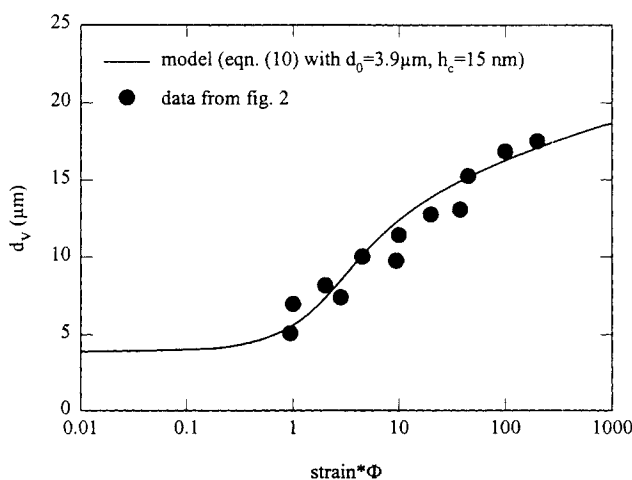


**Figure 4. Comparison of the model prediction of droplet-size evolution (Eq. 10) and the experimental coalescence results for a 10/90 blend (data of Figure 2).**

the results in Figure 1, yields  $h_c = 150$  nm, which is 25% lower than their value. Nevertheless, a difference of 25% in  $h_c$  gives less than 10% shift in the corresponding predictions for the steady-state droplet sizes. This discrepancy of 10% in the pseudo-steady-state droplet size can be attributed to the arbitrariness inherent in the determination of the pseudo steady state (see Eq. 7).

In all experiments shown in Figure 3 the initial droplet size almost satisfies  $d_0 \propto \dot{\gamma}_0^{-3/5}$ , since the initial shear rates that have been applied in these tests are either below the critical value or only slightly above it. Therefore, it has been verified whether Eq. 12 applies here. This equation, which gives the relative size increase of the disperse phase as a function of time, only contains a single parameter  $c$ . This parameter has been determined by fitting Eq. 8 through the pseudo-steady-state data (see Figure 1), using  $h_c = 15$  nm for the calculation of  $m$ . By doing so, a value of  $c = 2.4$  is obtained for the 10/90 blend. The resulting model curves for different ratios of initial over final shear rate are added in Figure 3. Good agreement is observed between the experimental results and the model curves. It is concluded that the proposed coalescence model can be used to predict both the absolute droplet size as a function of time (Eq. 10) as well as the relative droplet growth (Eq. 12). For the former, the values of the initial droplet size and of  $h_c$  are needed, whereas the latter only contains one adjustable parameter. Once this information is known for a particular blend and concentration, the morphology evolution due to coalescence can be predicted under various shear rates and step-down ratios.

Up to now the effect of blend concentration on the coalescence kinetics has not been discussed. Concentrations ranging from 2.5% to 20% PIB have been explored here to investigate the effect of this important parameter. A typical result is given in Figure 5, which shows the increase in droplet size after a step-down from 3 to 1  $s^{-1}$  for four different compositions. The data for the 2.5/97.5 and 5/95 blends result from microscopy; the 20/80 blend was studied rheologically. The 10/90 blend has been investigated with both techniques, and

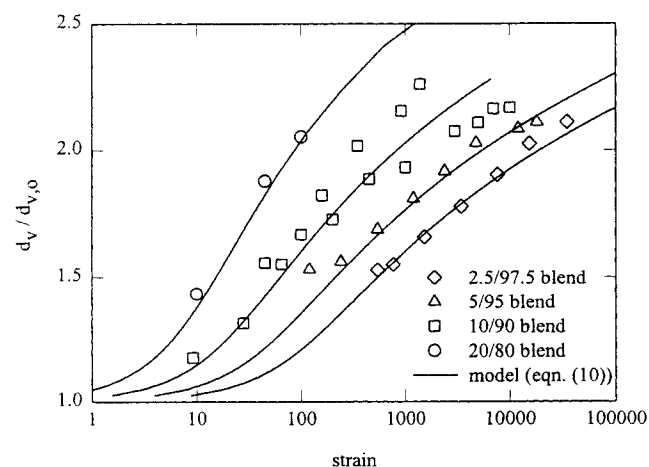


**Figure 5. Droplet-size evolution after a step-down from 3 to 1  $s^{-1}$  for blends with different concentration of disperse phase.**

The model curves are calculated with Eq. 10 using a concentration-dependent value for  $h_c$ : 12, 13, 15 and 60 nm for the 2.5/97.5, 5/95, 10/90 and 20/80 blends respectively.

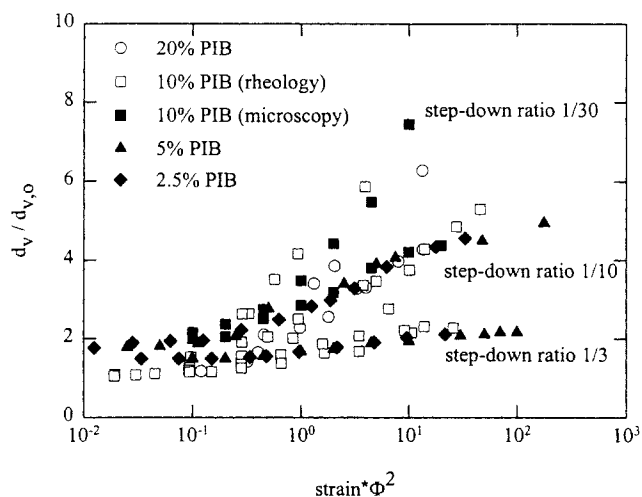


**Figure 6. Master curves, depending on the step-down ratio, for step-down experiments at different levels of shear rate and for different concentrations.**

The filled symbols represent microscopy results, whereas the open symbols are obtained by rheological measurements.

the agreement is satisfactory considering that 1  $s^{-1}$  is the limit for microscopic morphology analysis. For the sake of clarity, the overestimated initial values of droplet size, resulting from microscopy, are not shown. At a fixed shear rate, the coalescence process slows down considerably when the blend concentration decreases. The experimental data seem to indicate that the time scale for coalescence is proportional to the inverse of the fraction of droplet phase squared. Indeed, when the coalescence data are plotted as a function of strain, after step-down, multiplied by the square of the blend concentration, the data for the different blends can be superimposed, as shown in Figure 6.

The role of concentration in the model is not so obvious. At first glance, Eq. 10 seems to predict that the coalescence kinetics are a linear function of blend concentration. However, the parameter  $h_c$ , which appears through  $m$  on the left-hand side of Eq. 10, can depend on concentration. Introducing the concentration in  $h_c$  is a way of accounting for the effects of hydrodynamic interaction between the droplets that were neglected in the model. By adjusting the value of  $h_c$ , the model curves can be fitted nicely through the experimental data of Figure 5 for each concentration. Different values for  $h_c$  are obtained: they range from 12 nm for the most dilute blend (2.5/97.5 blend) to 60 nm for the most concentrated one (20/80). The increase of  $h_c$  with concentration of the disperse phase is similar to the findings of Minale et al. (1997b). These authors explain the effect of concentration by a reduced possibility for the droplets to escape from the contact zone during collision. Therefore there will be more collisions that actually lead to coalescence, which is reflected in the model by an increasing value for  $h_c$ .

Another possible explanation for the concentration dependence of  $h_c$  can be deduced from the work of Janssen (1993): he observed that if in a line of droplets two drops coalesce, the probability for further coalescence in their neighborhood is enhanced. This zipper effect can be ex-

plained as follows. If two droplets are pressed together they will not easily coalesce because the flattening of the interfaces yields a large contact area over which the matrix fluid has to drain. However, if these droplets are slightly moved apart, for example, due to the flow caused by coalescence events in their neighborhood, they become less flattened and can coalesce more easily since the drainage distance has decreased. Janssen made these observations for coalescence at rest, but this cooperative coalescence can be expected to occur in sheared systems as well. The preceding effects can be expressed, although somewhat artificially, by a concentration-dependent  $h_c$ . This simplifying approach works for the semidilute blends investigated here; nevertheless it is probably bound to fail for systems of high concentration. It should be noted also that, even with the concentration-dependent values for  $h_c$ , the model does not predict a scaling with strain multiplied with concentration squared. The experimental data are not conclusive on this point: although they can be roughly scaled by multiplying the strain with the concentration squared, subtle differences between the droplet size evolution in blends with different concentrations, predicted by the model, could be present as well.

In all the tests discussed so far only coalescence occurred because the capillary number remained below the critical value for breakup. As a final issue, the effect of a competitive breakup process on coalescence is considered. For that purpose a step-down experiment is presented where the final shear rate is larger than  $\dot{\gamma}_c$ , that is, where the breakup limit is smaller than the one for coalescence. It can be imagined that, under these conditions, initially solely coalescence will occur, but that after a certain increase in droplet size breakup will limit further droplet growth. Figure 7 shows a step-down experiment from  $3 \text{ s}^{-1}$  to  $1 \text{ s}^{-1}$  for the 20/80 blend. For this blend, the breakup limit at  $1 \text{ s}^{-1}$  is  $14.2 \mu\text{m}$ , as derived from the critical capillary number. This is below the maximum attainable droplet size for coalescence. Initially the droplet-size evolution seems only governed by coalescence, as can be deduced from the correspondence between the experimental results and the predictions of the coalescence model. How-

ever, when the droplet diameter becomes comparable to the breakup limit, no further increase is observed.

## Conclusions

The evolution of the droplet size after a sudden decrease in shear rate has been studied by means of rheological and microscopic measurements. By an appropriate choice of the test conditions, coalescence could be investigated without the interference of breakup processes. The effect of shear rate and concentration on coalescence has been studied in this manner for a model system. A coalescence model has been derived to describe the experiments, based on the approach suggested by Chesters (1991). The model predicts that the effect of flow conditions on coalescence kinetics can be expressed with only two dimensionless parameters: strain and step-down ratio. This is confirmed by the experiments. All material parameters being fixed, it is observed that blend concentration strongly affects the coalescence process: the time scale for coalescence seems inversely proportional to the fraction of droplet phase squared. Consequently, a master curve for each step-down ratio has been obtained by plotting the relative increase in droplet size vs. the strain after step-down multiplied by the square of the concentration.

## Acknowledgments

This work was partly supported by the European Community (Contract No. BRE2.CT92.0213), Onderzoeksfonds K.U. Leuven, FKFO (Belgium), and the Ministero dell'Universita e della Ricerca Scientifica e Tecnologica, Italy (60% funds). One of the authors (I.V.) is indebted to the FWO-Vlaanderen for a scholarship. The authors also thank Professor J. Mewis for useful discussions.

## Literature Cited

- Chesters, A. K., "The Modelling of Coalescence Processes in Fluid-Liquid Dispersions: A Review of Current Understanding," *Trans. Inst. Chem. Eng.*, **69**, 259 (1991).
- Doi, M., and T. Ohta, "Dynamics and Rheology of Complex Interfaces: I," *J. Chem. Phys.*, **95**, 1242 (1991).
- Elmendorp, J. J., and A. K. Van der Vegt, "A Study on Polymer Blending Microrheology: Part IV. The Influence of Coalescence on Blend Morphology Origination," *Poly. Eng. Sci.*, **26**, 1332 (1986).
- Grace, H. P., "Dispersion Phenomena in High Viscosity Immiscible Fluid Systems and Application of Static Mixers as Dispersion Devices in Such Systems," *Chem. Eng. Commun.*, **14**, 225 (1982).
- Grizzuti, N., and O. Bifulco, "Effects of Coalescence and Break-Up on the Steady State Morphology of an Immiscible Polymer Blend in Shear Flow," *Rheol. Acta*, **36**, 406 (1997).
- Janssen, J. M. H., "Dynamics of Liquid/Liquid Mixing," PhD Thesis, Eindhoven University of Technology, Eindhoven, The Netherlands (1993).
- Janssen, J. M. H., and H. E. H. Meijer, "Dynamics of Liquid-Liquid Mixing: A 2-Zone Model," *Poly. Eng. Sci.*, **35**, 1766 (1995).
- Minale, M., P. Moldenaers, and J. Mewis, "Effect of Shear History on the Morphology of Immiscible Polymer Blends," *Macromol.*, **30**, 5470 (1997a).
- Minale, M., J. Mewis, and P. Moldenaers, "Study of the Morphological Hysteresis in Immiscible Polymer Blends," *AIChE J.*, in press (1997b).
- Palierne, J. F., "Linear Rheology of Viscoelastic Emulsions with Interfacial Tension," *Rheol. Acta*, **29**, 204 (1990).
- Sigillo, I., L. di Santo, S. Guido, and N. Grizzuti, "Comparative Measurements of Interfacial Tension in a Model Polymer Blend," *Poly. Eng. Sci.*, **37**, 1540 (1997).
- Smoluchowski, M. von, "Versuch einer Mathematischen Theorie der Koagulationskinetik Kolloider Lösungen," *Z. Phys. Chem.*, **92**, 129 (1917).

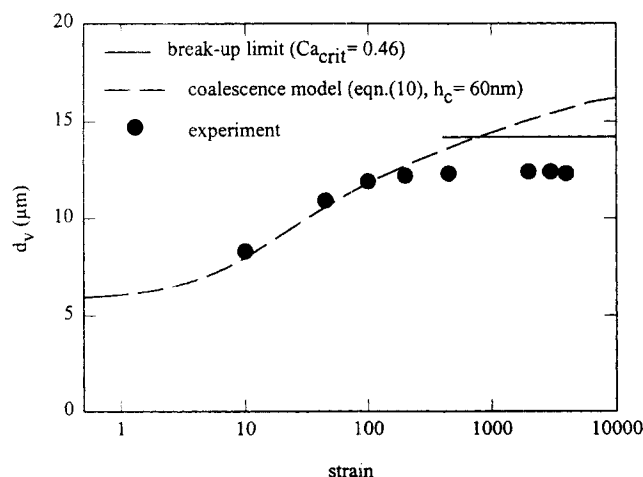


**Figure 7. Test where breakup processes take over after the initial coalescence-induced droplet growth (step from  $3$  to  $1 \text{ s}^{-1}$  for the 20/80 blend).**

The model curve for coalescence (Eq. 10) and the limit due to breakup are added for reference.

Søndergaard, K., and J. Lyngaae-Jørgensen, "Coalescence in an Interface-Modified Polymer Blend as Studied by Light Scattering Measurements," *Polymer*, **37**, 509 (1996).

Vinckier, I., P. Moldenaers and J. Mewis, "Relationship Between Rheology and Morphology of Model Blends in Steady Shear Flow," *J. Rheol.*, **40**, 613 (1996).

## Appendix

Before Eq. 2 can be integrated, the different terms in this equation should be given in an explicit form, containing only material parameters, shear rate, and droplet diameter. In the case of a uniform spherical morphology, the specific interfacial area is a function of the diameter  $d(t)$  and the volume fraction  $\phi$  of the droplets:

$$Q(t) = \frac{6\phi}{d(t)}. \quad (\text{A1})$$

The collision frequency, given by Eq. 3, can be rewritten as

$$C(t) = \frac{24\phi^2\dot{\gamma}}{\pi^2 d(t)^3} \quad (\text{A2})$$

by replacing the number of droplets per unit volume,  $n(t)$  in Eq. 3, by an expression in droplet size and volume fraction. The change in interfacial area due to a single coalescence event,  $\Delta S$ , can be obtained by subtracting the area of two small droplets from the area of one large droplet with a volume equal to that of the two small drops together:

$$\Delta S = -\pi d(t)^2(2-2^{2/3}). \quad (\text{A3})$$

In the expression for the drainage probability, Eq. 1, the drainage time for partially mobile interfaces will be used:

$$t_{\text{drain}} = \frac{\pi\eta_d F^{1/2}}{2[4\pi\alpha/d(t)]^{3/2}} \cdot h_c^{-1}, \quad (\text{A4})$$

where  $\eta_d$  is the viscosity of the disperse phase,  $\alpha$  the interfacial tension, and  $h_c$  the critical film thickness, as explained in the article. For the contact force  $F$ , the following estimate will be used (Janssen, 1993):

$$F = \frac{3}{2} \pi \eta_m \dot{\gamma} d(t)^2. \quad (\text{A5})$$

As mentioned in the article, the interaction time in Eq. 1 is set as the inverse of the shear rate. Introducing all these expressions into Eq. 2, yields a differential equation:

$$\frac{dd(t)}{dt} = \frac{4}{\pi} (2-2^{2/3}) \phi \dot{\gamma} d(t) \exp \left[ -\sqrt{\frac{3}{2}} \left( \frac{\eta_m \dot{\gamma}}{\alpha} \right)^{3/2} \frac{pd(t)^{5/2}}{16h_c} \right], \quad (\text{A6})$$

with  $\eta_m$  the matrix viscosity and  $p$  the viscosity ratio. When the parameter,  $m$ , defined in Eq. 6, is introduced and the numerical factors are combined, the preceding equation reduces to Eq. 5.

*Manuscript received Sept. 11, 1997, and revision received Jan. 20, 1998.*